Modification of Optical, Electronic and Microstructural Properties of PET by 150 keV Cs+ irradiation

Michał Musiatowicz[1], Marcin Turek[1], Andrzej Droździel[1*],
Krzysztof Pyszniak[1], Wojciech Grudziński[1]

[1] Institute of Physics,Maria Curie-Skłodowska University, Pl. M. Curie-Skłodowskiej 1, 20-031 Lublin, Poland
* Corresponding author's e-mail: adrozdzowa@o2.pl

ABSTRACT

Thick (0.125 mm) sheet samples of PET were irradiated with 150 keV Cs+ ion beam with fluences in the range from 10^{13} cm^{-2} up to 10^{16} cm^{-2}). Raman and UV-VIS spectroscopy measurements shown destruction of numerous bonds within the polymer – this effect intensifies with fluence. Raman spectroscopy shows the presence of amorphous graphitelike structures as the broad G band appears in the collected spectrum. The analysis of absorbance spectra also confirms formation of numerous carbon clusters leading to a formation of vast conducting structures in the modified layer of the polymer. One can observe the decrease of optical bandgap from 3.85 eV (typical for pristine PET) to 1.05 eV for the sample implanted with the highest fluence, the effect is weaker than for lighter alkali metal ions. The estimated average number of C atom in a clusters reaches in such case values close to 1100. The changes in the polymer structure lead to intense reduction of electrical sheet resistivity of the modified samples by ~ 8 orders of magnitude in the case of severely modified sample. The dependence of resistivity on temperature has also been measured. The plots of $\ln(\sigma)$ vs $1/T$ show that band conductivity or nearest neighbor hopping between conducting structures prevail in the considered case

Keywords: polymer modification, PET, ion implantation, FTIR and Raman spectroscopy, conducting layers.

INTRODUCTION

Polymers attract attention of engineers and scientists as they offer a multitude of superior properties very often enhanced by a possibility to compose them into a novel materials. As they are relatively strong, lightweight, weather- and corrosion resistant, economic and easy to form and posses desirable optical and electronic properties [1–3] various polymers are used in optics and microelectronics (e.g for sensors), in automotive industry, for production of a variety of coatings, for food packaging and last but not least as a biocompatible materials for medical implants.

A variety of techniques is used to change structural, physical and chemical properties of polymers: heat and laser light treatment, doping, ion beam mixing as well as irradiations with electron, ion, neutron or gamma ray beams [4–9]. Ion implantation is one of the most popular methods allowing tranformation of the thin upper layer of the synthetic material and change its often unpredictable electrical properties [10] making these these materials (usually characterised by very high resistance) much more applicable in electronic industry. It should be mentioned that properties of the modified layer are highly dependent on ion implantation processing parameters, such as irradiation fluence, the mass of the projectile and the irradiation current density.

The bombardment by energetic ions induces several interactions with target atoms leading to a plethora of phenomena including: chain scission and polymer degradation, electron excitation and ionisation, production of free radicals, polymer degassing and the formation of carbon–carbon bond based structures (carbonization) [11–14]. The impinging ions lose their energy to target

atoms due to two types of processes: (a) nuclear and (b) electronic stopping [15, 16]. Nuclear stopping mechanism involves elastic collision to transfer momentum and energy to host material, leading to bond breaking. chain scission and, consequently, polymer degradation. On the other hand electronic stopping occurs while projectiles interact via e.g. glancing inelastic collision with target atoms. The electronic stopping results in excitation of low-energy orbital electrons to high energy levels and could even lead to ionization of atoms [17]. As a large number of free radicals is produced via electronic stopping intense cross-linking of polymer is observed while this stopping mechanism dominates. In other words the ratio of nuclear and electronic stopping powers (Sn/Se) determines the path the structural modification of ion beam irradiated polymer will follow [18].

A plethora of ion implanted polymers were investigated over last decades, to mention only the most important ones including polyurethane [19], polystyrene [20], polyethylene [21], and polymethylmethacrylate (PMMA) [22]. An implanted polyethylene terephthalate (PET), also known as Mylar, Dacron, Terylene or Lawsan, gained special attention [23–27].

Due to its properties like high transparency, strength and resistance to harsh environment PET is widely used in various branches of industry for packaging (also of food), photovoltaics and other electronics, prosthetic medicine etc. It can be also a good base for high strength polymer blends [28] However, its large resistivity may e.g limit its application in electronics industry. One of the most popular ways to make it more conductive is ion implantation- formation of carbon cluster in the near-surface layer due to ion bombardment leads to dramatic decrease of resistivity by several orders of magnitude [29–32]. This structural change could be also easily seen a darkening of the initially transparent polymer, due to modification of the band structure leading also to the bandwidth reduction to values typical for semiconductors.

The aim of the current paper is checking properties of the modified polymer in the case of irradiation with very low projectile range, typical for heavy ion like Cs$^+$. The projected range is much shorter that the thickness of the polymer sheet. Hence, it is not possible to induce changes of the polymer structure that lead e.g. to the changes of resistivity also on the reverse side, as it was seen in the case of very thin foil (3 micrometers) and lighter projectiles [30,31]. One may expect that

the sample characterized by the thickness larger by more than two orders of magnitude is more resistant to changes induced by radiothermolysis occurring during ion bombardment. Changes of irradiated polymer microstructure investigated using both FTIR and Raman spectroscopies. Optical properties i.e. absorption in the UV-ViS is also under consideration. A special attention is given to modification of the optical bandgap related due to changes induced to polymer and emergence of new energy levels. One may expect that these changes will result in decrease of polymer surface resistivity – corresponding are also shown and discussed in the paper as well as results of measurements of the dependences of polymer conductivity on temperature. Such investigations should give some knowledge about the mechanism of conductance in the considered samples.
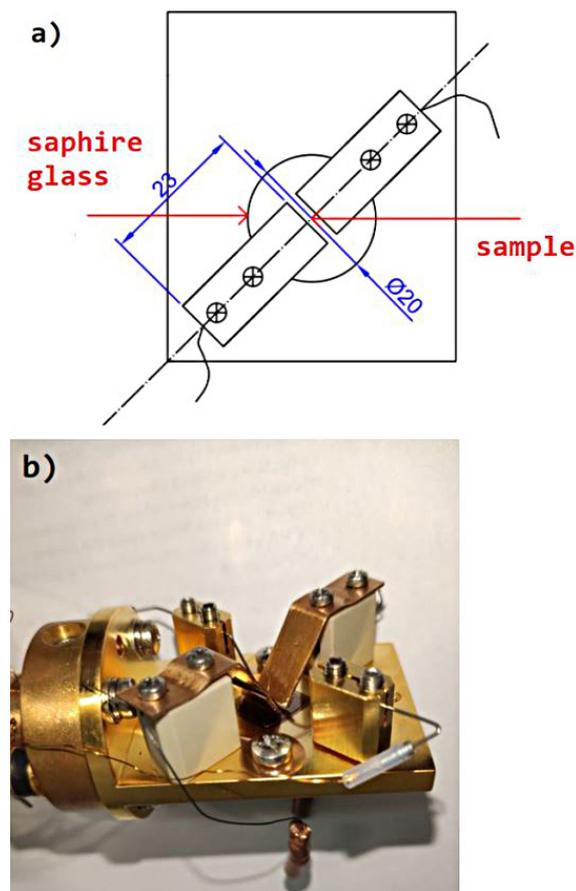
EXPERIMENTAL

Samples (5 cm x 5 cm) of transparent PET polymer sheet (thickness 0.125 mm, density ~1.4 g/cm^3) provided by Goodfellow were irradiated with 150 keV Cs ion beam. The ion beam was produced using CsCl as a feeding substance and plasma discharge ion source with internal evaporator described in details in [33,34]. Irradiations were performed with fluences 10^{13} cm^{-2}, 10^{14} cm^{-2}, 10^{15} cm^{-2} and 10^{16} cm^{-2}. The bombarding current density was kept at level up to 0.5 μA/cm^3 in order to avoid excessive sample heating. The sample was attached to sample holder using carbon adhesive tape, no additional supporting rings were used.

Depth distribution of the implanted Cs as well as the imposed damage were simulated employing SRIM software [35]. The simulation results are presented in Fig. 1. The ion average range was only ~100 nm with the 20 nm strangling. However one may expect that real Cs range could be at least 2 times larger having in mind results presented in [31] for Na implanted PET and then investigated with SIMS-TOF spectroscopy. In other words, one should be rather suspicious to the SRIM predictions in the case of polymer target bombardment. SRIM simulations results suggest that the depth of modified layer is approximately 100 nm but having in mind a plenty of processes during ion implantations in polymers its real thickness is larger, still by far less than the thickness of the sample.
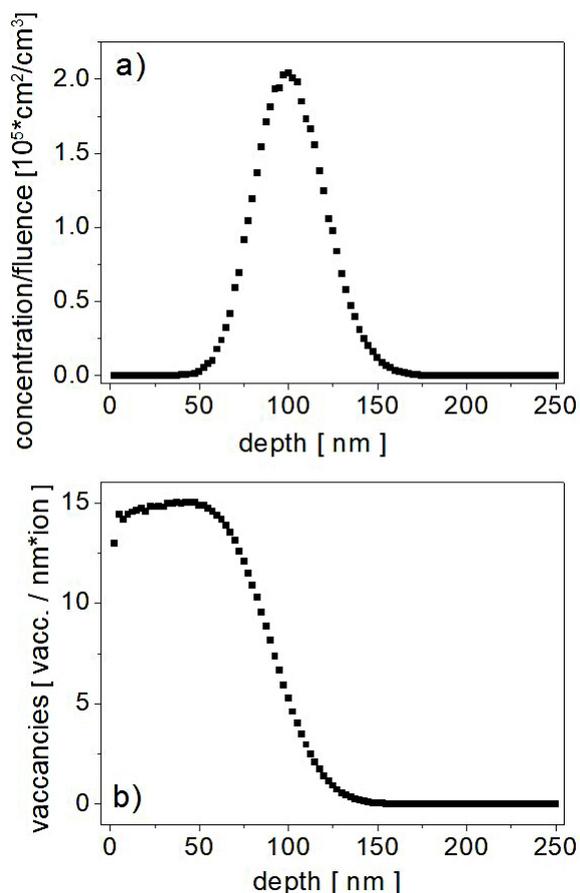
Figure 1. Cesium atoms (a) and vacancy (b) depth profiles for 150 keV Cs^+ implantation calculated using SRIM package

Figure 2. The geometry (a) and general view (b) of the electrode set used for measurements of resistivity as function of temperature
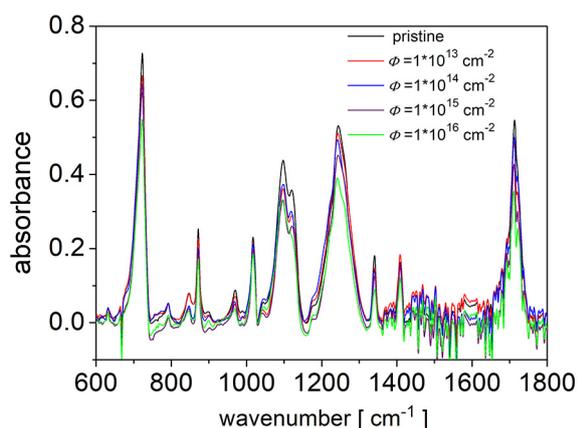
Absorption spectra in near UV and VIS regions were collected using Agilent Cary 50 spectrometer). FTIR-ATR (Fourier Transform Infra-Red Attenuated Total Reflectance spectrometry) measurements were performed employing Thermoscientific Nicolet iS50R spectrometer with GladiATR adapter. Raman spectra were obtained using Renishaw inVia system, using 514 nm excitation laser. Surface sample resistivity were measured using the Agilent B2911A measuring source and the set of polished electrodes of circular geometry. The dependences of sample resistivity on temperature were determined using Hioki 7110 megohmmeter. The samples were placed inside Janis VPF-100 cryostat, their temperature was governed by LakeShore model 325 temperature controller. Figure 2 shows custom electrode set made of phosphor bronze. The set was placed inside the cryostat chamber. In order to increase the measurement detection level and precision all devices were powered using separating transformer and additional filter.

RESULTS

It is commonly known that the way the polymer structure is modified by ion irradiation strongly depends on the stopping mechanism in the target [15, 16]. In the considered case of heavy 150 keV Cs^+ ions the dominant mechanism is the nuclear stopping – the S_n/S_e ratio is 7.8 at the surface and increases up to ~20 as the ion slows down. the total percentage of energy lost due to the electronic stopping is more than 92 % according to detailed SRIM simulations. Consequently, the strong effect of bond breaking, chain scission and polymer degradation should be expected. The destruction of chemical bonds in irradiated samples is well visible in FTIR spectra shown in Figure 3 especially for C=O bonds (stretching mode at ~1715 cm^{-1}) C-O (stretching at ~1240 cm^{-1} and 1120 cm^{-1}). The last peak is also combined with in-plane C-H bending mode at ~1123 cm^{-1}. Very strong reduction is also visible for out-of-plane C-H bending at 730 cm^{-1}). Similar but not as

Figure 3. FTIR spectra of
Cs⁺-implanted PET samples

Figure 4. Raman spectra for PET samples
implanted with Cs⁺. Dotted line marks the
position of the G band in graphite

strong decrease is observed also for 1330 -CH_2 waggling and 1018 cm^{-1} -CH in plane bending. One can however, see that the described effects measured using ATR-FTIR are more subtle than in the case of thinner foils, for which transitional FTIR measurements were applied. In the considered case the thickness of modified layer (even taking into account) is by far less than the thickness of the sample.

Evolution of microstructure of the implanted polymer could be also seen at Raman spectra shown in Figure 4. This change is much more subtle than in the case of lighter projectiles, having larger projected range. One can observe the decrease of the most prominent peaks at 1727 cm^{-1} and 1613 cm^{-1} corresponding to C=O and C=C in-ring stretching, respectively. It should be stressed that these peaks are well-visible even for relatively large fluence of 10^{15} cm^{-2}, and even for the most severely modified sample there are remnants of them. The other visible peaks are C-C-C in-plane aromatic ring bending (~630 cm-1), aromatic ring breathing mode (857 cm^{-1}) C-O stretching and C-H in plane bending (1097 cm^{-1} and 1118 cm^{-1}) and complex mode near 1286 cm^{-1} (ring and O-C stretching). All of them could be recognized up to the fluence of 10^{15} cm^{-2}, but disappear only for the sample irradiated with the largest fluence. It should be stressed that for lighter projectiles these peaks disappear for fluences at least one (Li⁺) and two (Na⁺ and K⁺) orders of magnitude smaller than in the current case. This may be caused by the fact the depth of the modifier layers is significantly smaller in that case and for smaller fluences the Raman signal from the deeper (unmodified) layers of the sample is collected. It should be noted that for fluence 10^{15} cm^{-2} the wide band
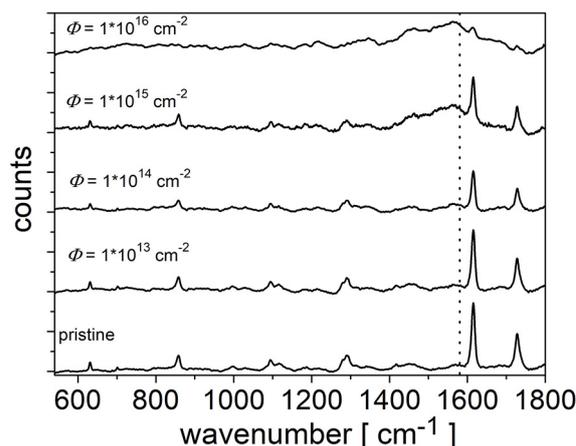
with the center near ~1580 cm^{-1} (marked with dotted line in Figure 4) appears. This band (called G band) is a fingerprint of graphitelike structures. In the case of Cs⁺ bombardment the formation of bands from the graphitelike structures is rather subtle – note that the D band near 1350 cm^{-1} is invisible. Anyway the formation of vast structures made of C atoms in sp2 hybrydisation is a characteristic feature of irradiated polymers [15, 24, 25, 36]. This transformation is induced by both nuclear stopping leading in the considered case to intense chain scission as well as by electronic stopping i.e. excitations followed by ionization, bond breaking and formation of radicals. Both these processes are also accompanied by degassing, which was observed during irradiation, however, to a smaller degree than in the case of lighter projectiles. The low content of D band seems to suggest that the carbon structures are mostly formed by rings, however the centroid of that band is shifted from its value typical for pure graphite (1852 cm^{-1}) toward lower values of the wavenumber, pointing at some disorder of the formed structure. The low I_D/I_G ratio is somewhat surprising as there is generally observed that the amount of chain-based structures increases with the mass of the projectile. One may suspect that larger Cs⁺ fluences would be required to definitely confirm it – once again it should be stressed that degree of carbonization is surprisingly low compared to the samples investigated in our previous studies.

As it has been already mentioned the modification of the PET polymer by Cs bombardment seems less intense than in previously considered

cases of lighter alkali metal ions. One can see the darkening of irradiated samples but the intensity of that transformation is smaller than in [31]. Changes of the sample transparency was tested quantitatively using UV-Vis spectroscopy. Results for the 300 – 700 nm range are shown in Figure 5a. The pristine sample is almost perfectly transparent for the light in the visible and near UV range, above ~300 nm. One can see that the absorbance of modified samples increases with the implantation fluence as the content of conducting carbon structures made of sp^2 hybridised atoms gets higher. Nevertheless, the effects are smaller than in the case of Na$^+$ or K$^+$ but also inert gases ion irradiations [30]. The change of absorption spectra is due to the emergence of new energy levels in the bandgap caused by carbonization of the polymer and is common for irradiated polymers [22,37]. In the considered case the implantation fluences were too low to observe the saturation of absorption changes.

As it was already mentioned the changes of absorption spectrum is related to the modification of energy band structure. It is known that the bandgap (E_o) could be calculated from absorption spectra employing the Tauc's approach. As one deals in the considered case with indirect allowed transition the relationship between light energy $h\nu$ and absorption coefficient has the form of:

$$\alpha h\nu \sim (h\nu - E_o)^2 \qquad (1)$$

Consequently, the bandgap can be found by (a) plotting $(\alpha h\nu)^{1/2}$ vs $h\nu$ and (b) determining the interception of the linear part of spectrum and \energy axis. Tauc plots obtained for measured spectra are presented in Figure 5b.

The estimated bandgap values are also gathered in Table 1. As in the case of other irradiations one can observe the decrease of the bandgap from ~3.95 eV for pristine/unimplanted PET to 1.05 eV for the sample irradiated witt the largest fluence. It should be noticed, that the change of the bandgap for Cs implanted samples is slightly smaller than in the case of heavier projectiles for which bandgap values were much below 1 eV (0.55 eV for K$^+$ and 0.7 for Na$^+$ [30], both results for E=150 keV and fluence of 10^{16} cm^{-2}) the change of the bandgap is to the great extent determined by the concentration of η-bonds in the modified polymer
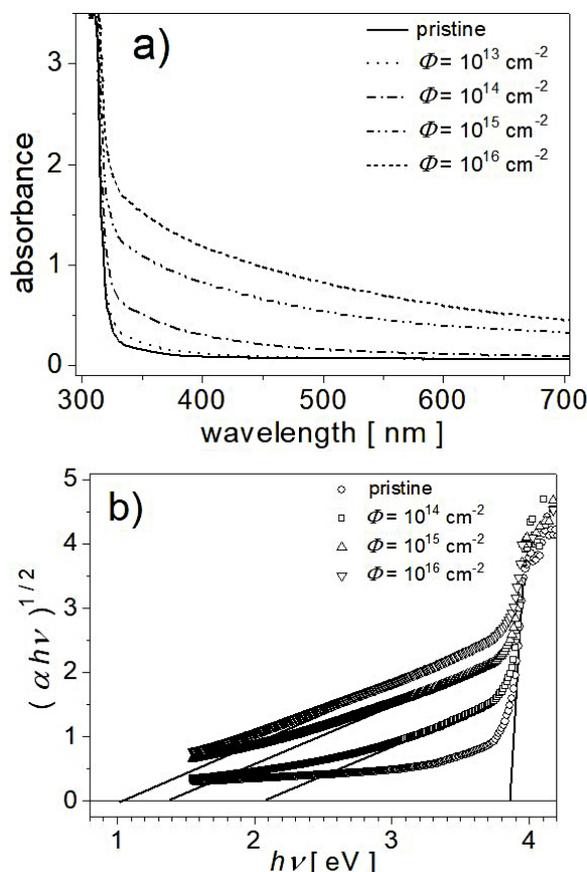

Figure 5. UV-VIS absorbance spectra (a) and Tauc plots (b) for the samples implanted with different Cs$^+$ fluences

Table 1. Optical bandgap energies (E$_o$) estimated using the Tauc approach and average carbon cluster sizes (N) for different Cs$^+$ irradiation fluences

Φ (cm^{-2})	E_o[eV]	N
0	3.85	-
1×10^{14}	2.1	267
1×10^{15}	1.4	600
1×10^{16}	1.05	1067

and, consequently, on the size of carbon clusters formed by sp^2 hybridised C atoms. The size of these clusters, or rather a number of C atoms they contain could be derived form absorption spectra [38,39]. The above mentioned number of carbon atoms (*N*) could be e.g. estimated according to a formula proposed in [39]:

$$N = \left(\frac{34.3}{E_o[eV]} \right)^2 \qquad (2)$$

The values of N obtained for Cs implanted PET sheets are shown in Table 1 along with E_o. As one may expect the size of the clusters rises fast with the irradiation fluence. Nevertheless, the average size of the carbon cluster cluster for maximal fluence (*N*=1067) is much smaller than that obtained for K$^+$ and Na$^+$ irradiated PET samples. However, it is twice as large as that estimated for 150 keV Li$^+$ bombarded PET foils.

Figure 6 presents relative surface resistivity of the PET polymer as function of the irradiation fluence. The resistivity decreases with fluence due to the formation of conducting carbon structures at the polymer surface. This effect is comparable to that observed for Na$^+$ irradiations [31] – the resistivity of sample implanted with the fluence 10^{16} Cs$^+$/cm^{-2} is almost 8 orders of magnitude smaller than that of the pristine sample. One deals with strong carbonization effect in the topmost layer of the polymer due to short projected range and the domination of the nuclear stopping in the case of the very heavy projectile.

The changes of samples resistivity with temperature were also under investigation. The measurements were done in temperature range from 300 K up to 500 K (or from the 380 K for pristine and most lightly irradiated sample) for the voltage between electrodes equal to 1000 V. Results are shown in Figure 7a. As one may expect the resistivity of both implanted an pristine samples decrease as the temperature of the sample rises.

The dependence of polymer conductivity on temperature could be written in the form [15]

$$\sigma = \sigma_o \exp\left(- \left(T_o/T\right)^m\right) \qquad (3)$$

where: T_o is some characteristic temperature parameter and σ_o is conductance for T tending to infinity. The power m is an indicator of conduction type. In the case of *m*=1 one deals most probably with band conduction in extended states or with nearest neighbor hopping conduction [40]. Higher values of *m* are related with variable range hopping mechanism between localized states in 1D, 2D or 3D structures with a relation of *m* and dimensionality *D*:
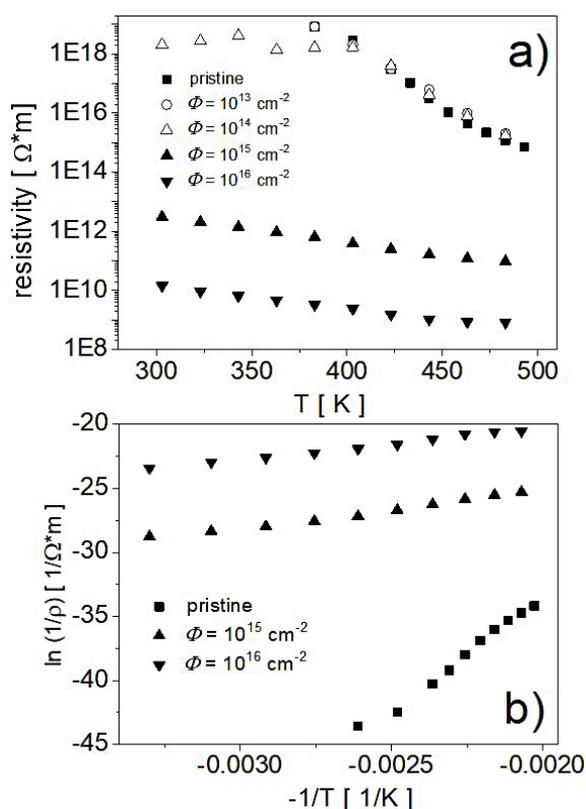
$$m = \frac{1}{1+D} \qquad (4)$$

Many irradiation-modified polymers exhibit *m*=1/2 dependence of conductance on temperature, and usually the dimensionality rises with the fluence [41, 42].

The dependence of ln(σ) on inverse temperature for selected samples are shown in Figure 7b. As one can see, in the considered case one deals with *m*=1, hence either the dominant conductance mechanism is the band conductance, or what is more probable for heavy modified polymer, a nearest neighbor hopping between conducting structures. It should be mentioned here that the case of *m*=1 is rare, but was also reported e.g. in [43].
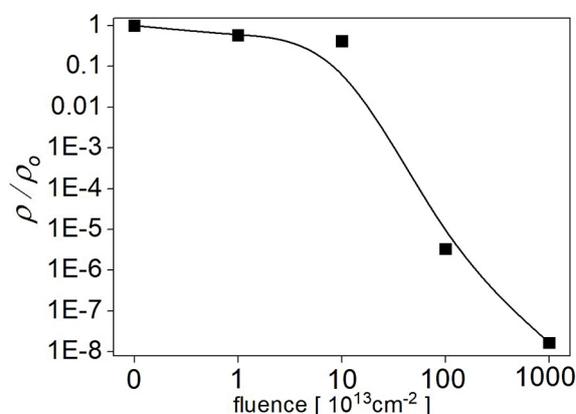
Figure 6. Sheet resistivity for Cs$^+$ implanted PET samples as function of fluence. The line is added just to guide the eye

Figure 7. Sheet resistivity of PET samples as function of temperature (a) ln (σ) vs. 1/T plots (b)

structures in the modified layer. Using the Tauc plot approach the reduction of the bandgap from ~3.95 eV (for pristine PET) down to 1.05 eV for the sample implanted with the maximal fluence is observed However, this effect is again not as strong as in the case of Na^+ or K^+ bombardment. As one may expect, the estimated size of carbon clusters is also smaller – it reaches ~1100 of C atoms for $\Phi=10^{16}$ cm^{-2}. All the above mentioned modifications of the polymer microstructure lead to the reduction of its electrical sheet resistivity. In the case of most heavily irradiated sample it decreases by approximately 8 orders of magnitude. The dependence of sample conductivity on temperature was also investigated in range up to 500 K. The obtained results suggest that the conductance model in he considered case involves mostly either band conductance or nearest neighbor electron hopping mechanism.

CONCLUSIONS

Changes of on microstructural, optical and electrical properties of PET in the form of 0.125 mm sheets due to 150 keV Cs^+ ion irradiation with fluences in the range from 10^{14} cm^{-2} up to $\times10^{16}$ cm^{-2}). Intensive breaking of numerous chemical bonds within the subsurface layer polymer is confirmed by Raman and UV-VIS spectroscopy and this effect rises with implantation fluence. The presence of broad G band in Raman spectra, which is known to be a sign graphitelike structures, confirms the formation of clusters made of sp^2 hybridised C atoms. This effect, however, needs larger fluences than in case of other alkali metal ions like, Na^+ or K^+. It should be noted that the D band could be barely seen in Raman spectra This, combined with the fact that G band center matches the position of original G band in graphite suggests that graphitelike structures are built mostly of carbon rings, unlike in the case of Na^+ or K^+ implantation, where the content of carbon atom chains was relatively large. The behaviour of UV-Vis absorbance spectra is a consequence of increasing size of carbon clusters culminating at formation of vast conducting

REFERENCES

1. Kosobrodova E., Kondyurin A., Chrzanowski W., McCulloch D.G., McKenzie, D.R., Bilek, M.M. Optical properties and oxidation of carbonized and cross-linked structures formed in polycarbonate by plasma immersion ion implantation. Nucl. Instrum. Methods Phys. Res. Sect. B Beam Interact. Mater. Atoms. 2014; 329: 52–63.

2. Charrier J.M. Polymeric Materials and Processing: Plastics, Elastomers, and Composites; Carl Hanser Verlag GmbH & Co, Munich, 1991.

3. Du W., Slaný M., Wang X. Chen G., Zhang J. The inhibition property and mechanism of a novel low molecular weight zwitterionic copolymer for improving wellbore stability. Polymers. 2020; 12: 708.

4. Akhtar A.N., Murtaza G., Shafique M.A., Haidyrah A.S. Effect of Cu Ions Implantation on Structural, Electronic, Optical and Dielectric Properties of Polymethyl Methacrylate (PMMA) Polymers. 2021; 13: 973.

5. Allayarov S.R., Olkhov Y.A., Dixon D.A., Allayarov R.S. Influence of Accelerated Protons on the Molecular–Topological Structure of Polyethylene, High Energy Chem. 2020; 54: 368–373.

6. Pirker L., Krajnc A.P., Malec J., Radulovi´c V., Gradišek A., Jelen A., Remškar M., Mekjavic I.B., Kovac J., Mozetic M. et al. Sterilization of polypropylene membranes of facepiece respirators by ionizing radiation. J. Membr. Sci. 2020; 619: 118756.

7. Tyutnev A.P., Saenko V.S., Zhadov A.D., Abrameshin D.A. Theoretical Analysis of the Radiation-Induced Conductivity in Polymers Exposed to Pulsed and Continuous Electron Beams, Polymers. 2020; 12: 628.

8. Przybytniak G., Kornacka E.M., Mirkowski K., Walo M., Zimek Z. Functionalization Of Polymer Surfaces By Radiation-Induced Grafting, Nukleonika. 2008; 53(3): 89–95.

9. Obilor A.F., Pacella M., Wilson A., Silberschmidt V.V. Micro-texturing of polymer surfaces using lasers: a review, The International Journal of Advanced Manufacturing Technology. 2022; 120: 103–135.

10. Wu Y., Zhang T., Liu A., Zhang X., Zhou G. The modification behaviour for Si implanted PET, Science in China E. 2003; 46: 125.

11. Dhillon R.K., Singh P., Gupta S.K., Singh S., Kumar R. Study of high energy (MeV) N6+ ion and gamma radiation induced modifications in low density polyethylene (LDPE) polymer. Nucl. Instrum. Methods Phys. Res. Sect. B Beam Interact. Mater. Atoms. 2013; 301: 12–16.

12. Cinan Z.M., Erol B., Baskan T., Mutlu S., Savaskan Yilmaz S. Yilmaz A.H. Gamma Irradiation and the Radiation Shielding Characteristics For the Lead Oxide Doped the Crosslinked Polystyrene-b-Polyethyleneglycol Block Copolymers and the Polystyrene-b-Polyethyleneglycol-Boron Nitride Nanocomposites, Polymers. 2021; 13: 3246.

13. Guenther M., Gerlach G., Suchaneck G., Sahre K., Eichhorn K.J., Wolf B., Deineka A., Jastrabik L. Ion beam induced chemical and structural modification in polymers Surf. Coat. Technol. 2002; 158–159: 108–113.

14. Rai V., Mukherjee C., Jain B. UV-Vis and FTIR spectroscopy of gamma irradiated polymethyl methacrylate, Indian J. Pure Appl. Phys. 2017; 55: 775–785.

15. Popok V. Ion implantation of polymers: Formation of nanoparticulate materials. Rev. Adv. Mater. Sci. 2012; 30: 1–26.

16. Mikšová R., Macková A., Pupikova H., Malinský P., Slepicka, P., Švorˇcík, V., Compositional, structural, and optical changes of polyimide implanted by 1.0 MeV Ni+ ions. Nucl. Instrum. Methods Phys. Res. Sect. B Beam Interact. Mater. Atoms. 2017; 406: 199–204.

17. Goyal P.K., Kumar V., Gupta, R., Mahendia S., Kumar S. Modification of polycarbonate surface by Ar+ ion implantation for various opto-electronic applications. Vacuum. 2012; 86: 1087–1091.

18. Sharma A., Chawla M., Gupta D., Bura M., Shekhawat, N. Aggarwal, S. Low energy B+ implantation induced optical and structural characteristics of aliphatic and aromatic polymers. Vacuum. 2019; 159: 306–314.

19. Morozov I.A., Mamaev A.S., Osorgina I.V., Lemkina L.M., Korobov V.P., Belyaev A.Y., Porozova S.E.,. Sherban,M.G., The modification behaviour for Si implanted PET. Structural-mechanical and antibacterial properties of a soft elastic polyurethane surface after plasma immersion N+2 implantation, Mater. Sci. Eng. C 2016; 62: 242–248.

20. Bilek M.M., Kondyurin A., Dekker S., Steel B.C., Wilhelm R.A., Heller R., McKenzie D.R., Weiss A.S., James M., Möller W. Depth-resolved structural and compositional characterization of ion-implanted polystyrene that enables direct covalent immobilization of biomolecules., J. Phys. Chem. C. 2015; 119: 16793–16803.

21. Nenadović M., Potocnik J., Ristić M., Strbac S., Rakocević Z. Surface modification of polyethylene by Ag + and Au + ion implantation observed by phase imaging atomic force microscopy Surface and Coatings Technology. 2012; 206: 4242–4248.

22. Kavetskyy T., Iida K., Nagashima Y., Kuczumow A., Šauša O., Nuzhdin V., Valeev V., Stepanov A.L. High-dose boron and silver ion implantation into PMMA probed by slow positrons: Effects of carbonization and formation of metal nanoparticles, J. Phys.: Conf. Ser. 2017; 791: 012028.

23. Djebara M., Stoquert J.P., Abdesselam M., Muller D., Chami A.C. FTIR analysis of polyethylene terephthalate irradiated by MeV He+, Nucl. Instr. Meth. 2012; B274: 70–77.

24. Goyal P.K., Kumar V., Gupta R., Mahendia S., Kumar S. Change in the Electrical Conductivity of N+ Ion Implanted Polycarbonate, Advances in Applied Science Research. 2011; 2(3): 227–231.

25. Kumar R., Goyal M., Sharma A., Aggarwal S., Sharma A., Kanjilal D. Effect of 200 keV Ar+ implantation on optical & electrical properties of polyethyleneterepthalate (PET), AIP Conf. Proc. 2015; 1661: 110010-1.

26. Sant'Ana P.L., Ribeiro J.R., da Cruz N.C., Rangel E.C., Durrant S.F., Costa Botti L.M., Rodrigues Anjos C.A., Azevedo S., Teixeira V., Silval C.I., Carneiro J., Medeiros E.A., de Fátima Soares N.F., Nanomed Nanotechnol. 2018; 3(3): 000145.

27. Chawla M., Rubi R., Kumar R., Sharma A., Aggarwal S., Kumar P., Kanjilal D. Tailoring Structural Properties of Polyethylene Terephthalate (PET) by 200 keV Ar+ Implantation. Advanced Materials Research. 2013; 665: 221–226.

28. Bocz K., Ronkay F., Decsov K.E., Molnár B., Marosi G., Application of low-grade recyclate to enhance reactive toughening of poly(ethyleneterephthalate), Polymer Degradation and Stability. 2021; 185: 109505.

29. Gohs U., Böhm R., Brünig H., Fischer D., Häussler L., Kirsten M., Malanin M.,. Müller M.-T, Cherif C., Wolz D.S.J., Jäger H. Electron beam treatment of polyacrylonitrile copolymer above the glass transition temperature in air and nitrogen atmosphere, Radiation Physics and Chemistry. 2019; 156: 22–30.

30. Droździel A., Turek M., Pyszniak K., Prucnal S., Luchowski R., Grudziński W., Klimek-Turek A., Partyka J., Modification of optical and electrical properties of PET foils by He+, Ne+ and Ar+ implantation, Acta Physica Polonica A. 2017; 132(2): 264–269.

31. Turek M., Droździel A., Pyszniak K., Luchowski R., Grudziński W., Klimek-Turek A.. Modification of PET Polymer Foil by Na+ Implantation Acta Physica Polonica A. 2019; 136(2): 278–284.

32. Turek M., Drozdziel A., Pyszniak K., Grudziński W., Klimek-Turek A. Modyfikacja właściwości folii PET przy wykorzystaniu naświetlania jonami K+ (in Polish) Przegląd Elektrotechniczny. 2020; 96(8): 151–155.

33. Turek M., Drozdziel A., Pyszniak K., Prucnal S. Versatile plasma ion source with an internal evaporator, Nucl. Instr. Meth. B. 2011; 269: 700–707.

34. Turek M., Drozdziel A., Pyszniak K., Prucnal S., Zuk J. Źródło jonów z parownikiem ogrzewanym przez wyładowanie łukowe. Symulacje komputerowe i eksperyment (in Polish). Przegląd Elektrotechniczny 86(7), 2010, 193–196

35. Ziegler J. F., Ziegler M. D., Biersack J. P., The Stopping and Range of Ions in Mater Nucl. Instr. Meth. B. 2010; 268: 1818–1823.

36. Sviridov D.V. Chemical aspects of implantation of high-energy ions into polymeric materials Russian Chemical Reviews. 2002; 71(4): 315–327.

37. Arif S., Rafique M. S., Saleemi F., Sagheer R., Naab F., Toader O., Mahmood A., Rashid R., Mahmood M. Influence of 400 keV carbon ion implantation on structural, optical and electrical properties of PMMA, Nucl. Instr. Meth. B. 2015; 358: 236–244.

38. Nouh S.A., Abdul-Salem M.H., Ahmed Morsy A. Electrical, optical and structural behaviour of fast neutron-irradiation-induced CR-39 SSNTD Radiat. Meas. 2003; 37(1): 25–29.

39. Gupta S., Choudhary D., Sarma A., Study of carbonaceous clusters in irradiated polycarbonate with UV–vis spectroscopy, J. Polym. Sci. B: Polym. Phys. 2000; 38(12): 1589–1594.

40. Wang Y., Mohite S.S., Bridwell L.B., Giedd R.E., Sofield C.J. Modification of high temperature and high performance polymers by ion implantation, J. Mater. Res. 1993; 8: 388–402.

41. Komarov F.F., Leontyev A.V., Grigoryev V.V. Electrophysical properties of organic materials irradiated with accelerated ions Nucl. Instrum. Meth. Phys. Res. B. 2000. 166–167: 650–654.

42. Chen T., Yao S., Wang K., Wang H., Zhou S. Modification of the electrical properties of polyimide by irradiation with 80 keV Xe ionsSurf. Coat. Technol. 2009. 203(24): 3718–3721.

43. Popok V.N., Karpovich I.A., Odzhaev V.B., Sviridov D.V. Structure evolution of implanted polymers: Buried conductive layer formation Nucl. Instrum. Meth. Phys. Res. B. 1999; 148(1–4): 1106–1110.